ACI STRUCTURAL JOURNAL TECHNICAL PAPER

Title no. 93-S60

Seismic Strengthening of Circular Bridge Pier Models with Fiber Composites



by H. Saadatmanesh, M. R. Ehsani, and Limin Jin

An experimental investigation was conducted to study the seismic behavior of reinforced concrete columns strengthened with fiber reinforced plastic (FRP) composite straps. Five concrete column-footing assemblages were constructed with a $^1/_5$-dimensional scale factor. The unidirectional glass fabric straps were impregnated with polyester resin and wrapped around the potential plastic hinge zone of the columns. An epoxy layer was applied to the straps while wrapping for interlaminar bond. All specimens were tested under inelastic reversal loading while simultaneously subjected to a constant axial load. Test results show that seismic resistance of retrofit concrete columns improves significantly as a result of the confining action of the FRP composite straps. The straps are highly effective in confining the core concrete and preventing the longitudinal reinforcement bars from buckling under cyclic loading.

Keywords: bridges; columns; confinement; ductility; fiber reinforced plastics (FRP); fiber composites; seismic behavior; seismic strengthening.

INTRODUCTION

The recent earthquakes in California and Japan have caused extensive damage to highway bridge structures. Failure of these structures exposed a number of structural deficiencies in many bridges and buildings constructed before the new seismic design codes were in place.[1] In particular, it has been demonstrated that concrete columns with inadequate lateral reinforcement contributed to the catastrophic collapse of many bridges. The poor detailing of the starter bars in these columns compounded the problem of seismic deficiency. The moments and lateral forces induced by seismic loads result in large shear forces in bridge columns, which are resisted mainly through lateral ties or spirals around the main reinforcement. The lateral reinforcement, if properly detailed and anchored, can also prevent sudden loss of bond and buckling of the longitudinal bars. Therefore, in columns with inadequate lateral reinforcement, it is imperative to provide additional external confinement to insure ductile behavior.

Many techniques that have been implemented into the retrofit design process have been based mainly on experimental testing of scaled-down models of bridge structures. Previous research[2,3] has indicated that closely spaced transverse reinforcement in the potential plastic hinge zone of bridge columns increases ultimate compression strength and strain of the concrete core. Recent tests conducted at the University of California at San Diego[4-7] have shown that strengthening bridge columns with steel jackets or with fiberglass/epoxy jackets significantly improves the flexural and shear strengths and increases the ductility of the column.

The primary objective of this paper is to present the results of an investigation on circular columns retrofit with FRP composite straps. Scaled-down concrete columns were wrapped with high- performance FRP composite straps and then tested under reversing inelastic load cycles. Glass fibers in the FRP composite straps were unidirectionally arranged and impregnated with polyester resin. A layer of epoxy was then brushed on the strap for interlaminar bond, while the strap was being wrapped around the column. The major design parameters in this study were the anchorage details of the column longitudinal steel and the retrofit scheme, i.e., providing passive or active confinement for the column.

RESEARCH SIGNIFICANCE

Many bridge failures during the recent earthquakes were caused by poor performance of concrete columns, primarily due to inadequate lateral reinforcement and insufficient lap length of the starter bars. The research presented in this paper provides an effective and economical alternative for seismic retrofitting of this type of substandard concrete columns. Furthermore, the results presented in this paper will provide an insight into new materials, such as fiber composites, for retrofitting and reinforcing of concrete structures.

SEISMIC RETROFITTING OF RC COLUMNS WITH FRP COMPOSITE STRAPS

The use of composite materials in the construction industry and infrastructure-related applications has significantly

ACI Structural Journal, V. 93, No. 6, November-December 1996.
Received May 30, 1995, and reviewed under Institute publication policies. Pertinent discussion will be published in the September-October 1997 *ACI Structural Journal* if received by May 1, 1997.

H. Saadatmanesh is Associate Professor in the Department of Civil Engineering and Engineering Mechanics, University of Arizona, Tucson, Arizona. He is Secretary of ACI Committee 440, FRP Reinforcement, and his primary research interests include application of fiber composites for strengthening and rehabilitation of structures.

M. R. Ehsani is Associate Professor in the Department of Civil Engineering and Engineering Mechanics, University of Arizona. He is a member of several ACI committees, including Committee 440, Fiber Reinforced Plastic Reinforcement, and he is a registered structural engineer in Arizona.

Limin Jin is a structural engineer with Ove Arup, Inc., Los Angeles, California. He received his PhD from the Department of Civil Engineering and Engineering Mechanics at the University of Arizona in May 1995. His research interests include earthquake-resistant design and application of fiber composites in structures.

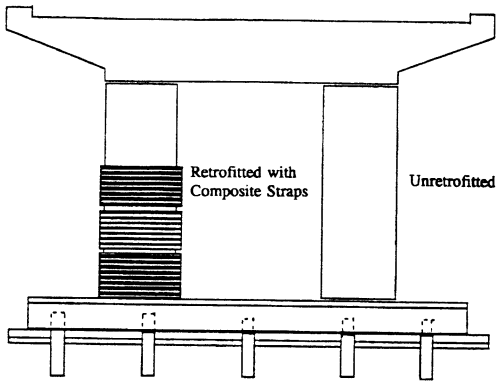

Fig. 1—Retrofit and nonretrofit concrete columns

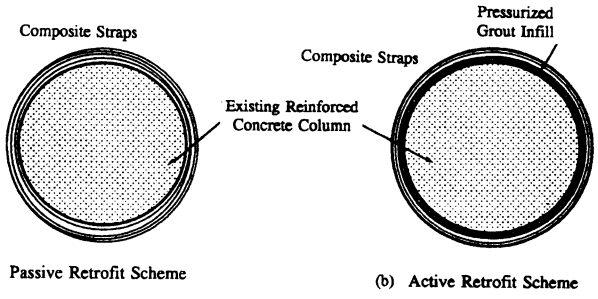

Fig. 2—Active and passive retrofit schemes

increased in recent years; the majority of these applications have been in corrosive environments to take advantage of the corrosion resistance of composites.[8] Fiber reinforced composites have long been recognized for their high-strength, good fatigue life, light weight, ease of transportation and handling, and low maintenance costs.

Fiber composites, in general, are constructed of filaments such as glass, kevlar, carbon, etc., embedded in a resin matrix. The fibers are the primary load-carrying elements within the composite. The matrix binds the fibers together and transfers loads between them. It also protects the fibers from environmental attack and damage due to handling. The fibers have a strong influence on mechanical properties of the composite, such as strength, elastic modulus, and deformation properties.

Glass fibers are the most common of all reinforcing fibers for resin-matrix composites. The principal advantages of glass fibers are the low cost and high strength. Fiberglass fabrics are one of the various forms of glass fibers that are commercially available and are very versatile for seismic retrofit applications. The fibers could all be oriented in one direction (unidirectional), or different amounts of fibers could be oriented in different directions to achieve an optimum structural performance in a desired direction. For the confinement of columns in this study, unidirectional tapes of E-glass were manufactured in the laboratory. These tapes were wrapped in multiple layers around the column to form external hoops for improved confinement. Fig. 1 shows an existing concrete bridge column wrapped with composite straps in the potential plastic hinge region.

Both active and passive retrofit methods were tested in the laboratory to show the effectiveness of different retrofit schemes for enhancing the shear and flexural behaviors. For the passive retrofit scheme, the composite straps with fiber orientation in the circumferential direction were directly wrapped onto the column in the region of the reinforcement lap splices and/or the potential plastic hinge zone, as shown in Fig. 2(a). In this case, as the concrete expands outward, tensile stresses are gradually developed in the composite straps that will resist this expansion; thus, the system is referred to as passive confinement. For the active retrofit scheme, the composite straps were slightly oversized for the column and the resulting gap between the column and the straps was initially injected with pressurized epoxy resin, as shown in Fig. 2(b). Spacers were provided between the column and the straps to maintain a uniform gap. This retrofit scheme induces initial tensile stresses in the straps. As a result, an active pressure is created around the column. This pressure reduces the amount of radial dilation and cracking of the core concrete.

EXPERIMENTAL PROGRAM

Test specimens

Test results for five scaled-down, circular reinforced concrete bridge column footing assemblages are reported in this paper. Test specimens were designed to approximately model typical pre-1971 design of existing highway bridge columns in a zone of high seismic risk. Each specimen consisted of a single column bent with strong footing details, as shown in Fig. 3. The composite strap was applied only in the potential plastic hinge region; i.e., in the 635-mm-(25-in.)-long portion of the column above the top face of the footing. Fig. 4 shows a typical column specimen wrapped with the composite straps in the plastic hinge region prior to the beginning of the test.

Materials used in the construction of the column specimens included concrete with $f_c' = 34.5$ MPa (5000 psi) and Grade 40 steel. Although the specific concrete compression strength for the prototype bridge column was 21 MPa (3000 psi), ready-mixed concrete providing $f_c' = 34.5$ MPa (5000 psi) was used to include the effect of expected overstrength resulting from normal conservative mix design and strength gain with concrete aging. The actual compression strength of the concrete for each specimen is given in Table 1.

The diameter of the columns was 305 mm (12 in.) These columns were reinforced longitudinally with 14 No. 4 bars [diameter = 13 mm ($^1/_2$ in.)], resulting in a longitudinal

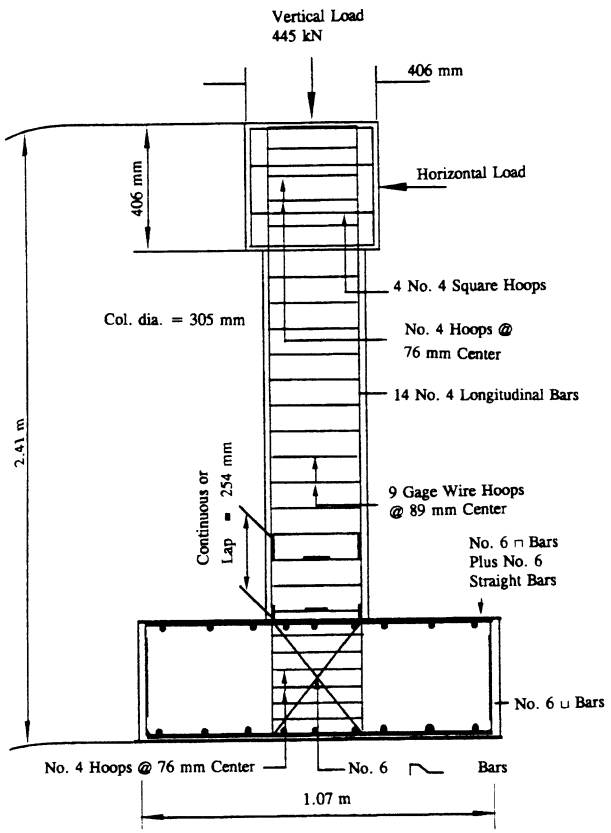

Fig. 3—Geometric details of column specimens

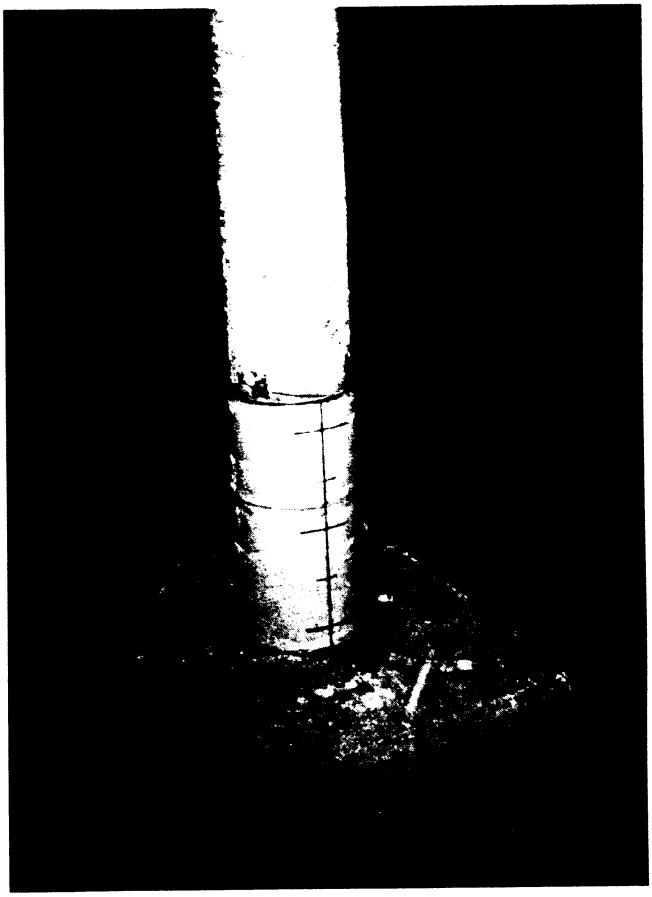

Fig. 4—Column wrapped with composite straps in plastic hinge region

reinforcement ratio of 2.48 percent. The measured yield strength for these bars was 358 MPa (53 ksi). Transverse confinement was provided by 9-gage steel wire [diameter = 3.5 mm (0.135 in.)] hoops spaced at 89 mm (3.5 in.) on center throughout the entire height of the column. The average yield stress for these wires was 301 MPa (43.7 ksi). The only difference among specimens was in the detail of anchorage of column longitudinal steel reinforcement and the type of confinement, i.e., passive or active (Table 1). For Specimens C-1, C-2, and C-3, the longitudinal reinforcement of the column was extended into the footing using starter bars that were lapped with the main longitudinal reinforcement of the column over a length of 20 bar diameters, i.e., 254 mm (10 in.). Columns C-2 and C-3 were strengthened using the passive and active retrofit scheme, respectively. For Specimens C-4 and C-5, the column reinforcement extended into the footing and was anchored with a standard 90-deg hook. Column C-4 was used as the control specimen, while Column C-5 was retrofit with the passive scheme.

The composite straps constructed for this project were 0.8-mm-(0.03-in.)-thick and had a tensile strength and modulus of elasticity of 532 and 18.6 GPa (77 and 2700 ksi), respectively. The stress-strain relationship of the composite strap was linear-elastic to failure. For both active and passive retrofit schemes, the columns were wrapped with six layers of FRP composite straps, resulting in a total thickness of 5 mm (0.2 in.) within the potential plastic hinge zone of the column, i.e., from the top of the footing to 635 mm (25 in.) above it. As the strap was wrapped around the column, an epoxy was applied to its surface and the multiple layers of the strap were adhered together to form a single composite wrap with the desired thickness. The epoxy was selected to insure that the multiple layers of the straps acted as one unit with no interlaminar slipage.

Table 1—Details of column specimens

Specimen	Measured concrete strength, MPa	Type	Longitudinal steel detail	Retrofit
C-1	36.5	Control	Starter bars	None
C-2	38.3	Retrofit 1	Starter bars	Passive
C-3	38.5	Retrofit 2	Starter bars	Active
C-4	36.6	Control	Continuous bars	None
C-5	36.5	Retrofit 1	Continuous bars	Passive

Test setup and instrumentation

The test setup was designed for testing column-footing assemblages subjected to combined axial and lateral loadings. The specimens were tested in a steel reaction frame, as shown in Fig. 5. Two independent loading systems were used to apply the load to the specimens. First, the axial load of 445 kN (100 kips) was applied to the column by prestressing a pair of 25-mm-(1-in.)-diameter high-strength steel rods against the base beams of the test frame, which was bolted to the 915-mm-(3-ft)-thick concrete floor. This load was applied to simulate the dead load on the columns. Next, the reversing lateral forces were applied to the column by an MTS ± 489 kN (± 110 kips) hydraulic actuator mounted on the reaction frame. The actuator was capable of moving the top of

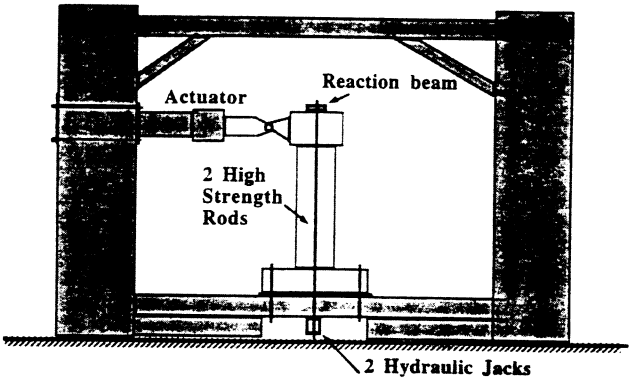

Fig. 5—Test setup

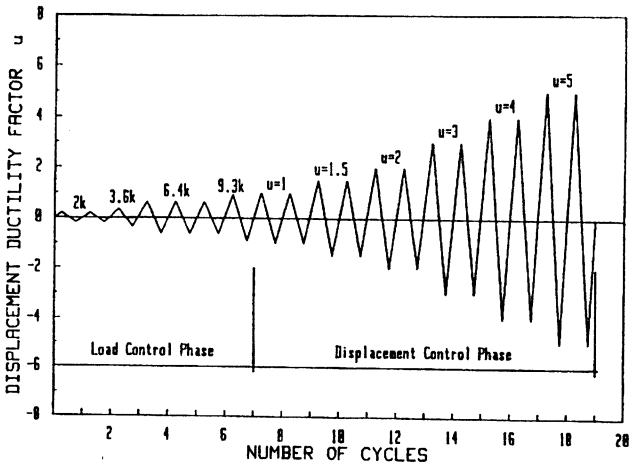

Fig. 6—Loading sequence

the specimen 127 mm (5 in.), in both positive and negative directions. A displacement of 127 mm (5 in.) corresponds to a drift of approximately 7 percent. Each column was instrumented to monitor the applied displacement and corresponding loads, strains, and deformations. Four types of instruments were used to measure the various quantities. These included:

a) The calibrated load cell and displacement transducer of the actuator.

b) The electrical inclinometers mounted on the potential plastic hinge region of the column to measure rotation.

c) The displacement transducers installed on the steel reference frame.

d) Electrical-resistance strain gages bonded to reinforcing bars.

e) Photographic records of the column cracking and failure modes.

The effect of an earthquake on the column specimen was simulated by reversed cyclic loading. The hydraulic actuator in the test setup was used to displace the top of the column to achieve a predetermined load level or displacement. Then, the loading direction was reversed to achieve the same load or displacement level in the opposite direction. The load and displacement input history was broken into two phases. At the initial stage, the test was in a load control mode. On yielding of the longitudinal reinforcing bars, a displacement control mode of loading was utilized; Fig. 6 shows the loading sequence. The letter "u" in this figure indicates the

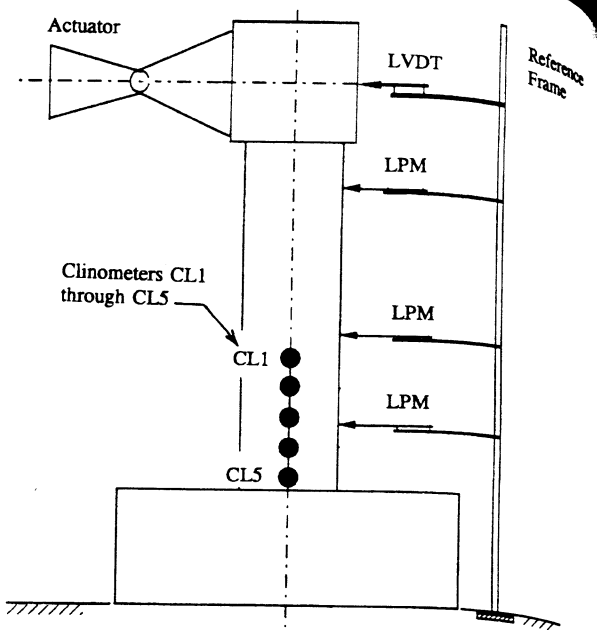

Fig. 7—Inclinometer and transducer arrangement

displacement ductility factor defined as the ratio of the applied displacement over the displacement at first yielding of the longitudinal reinforcing bars. The hysteresis loops of applied lateral loads versus the column free end displacement at the point of application of the load were continuously plotted and updated on the computer during the test.

Ten electrical inclinometers were distributed at 127 mm (5 in.) spacing over both opposite faces of the column within the plastic hinge region from the top of the footing up to a height of 635 mm (25 in.), as shown in Fig. 7. Data from these clinometers were used to measure the plastic hinge rotations at critical sections of the column and to plot the moment-curvature relationship of these sections. Along the height of the column, four displacement transducers were used to monitor the column deflection, as shown in Fig. 7.

The strains in the reinforcing bars at the locations within the plastic hinge zones of the column were measured by means of electrical resistance strain gages bonded to the steel bars. Twelve strain gages were bonded to the column bars and hoops. In addition, for each retrofit column, a total of 12 strain gages were attached to the composite straps to measure the hoop strains in the straps.

During each loading cycle, testing was stopped for a few seconds at several points while all data were scanned through a data acquisition system. Readings were automatically controlled and the data were stored on floppy disks.

Load-versus-displacement response

Plots of the lateral load-versus-displacement for all five specimens are shown in Fig. 8 through 12. It should be noted that these figures have been plotted to the same scale. Because the columns were symmetrically reinforced with respect to the positive and negative sides for each specimen, the resulting positive and negative portions of each specimen's hysteresis loops should be symmetrical and identical in values. However, due to a limitation of the hydraulic actuator, the maximum strokes reached in the positive and negative

Table 2—Measured and calculated strength of columns

Specimen	Calculated lateral load*, kN (nonretrofit)	Measured maximum lateral load, kN (retrofit)	Increase in strength resulting from retrofitting
C-1	50.7	58.3	Control
C-2	50.7	81.4	40 percent
C-3	50.7	89.4	53 percent
C-4	50.7	71.6	Control
C-5	50.7	87.2	22 percent

*Using ACI.

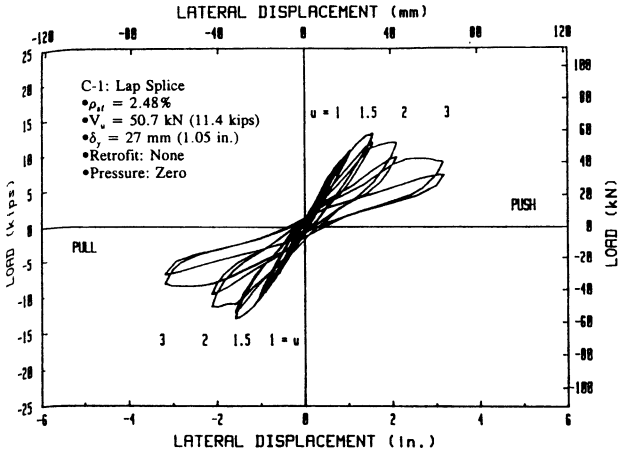

Fig. 8—Load-versus-displacement response of Column C-1

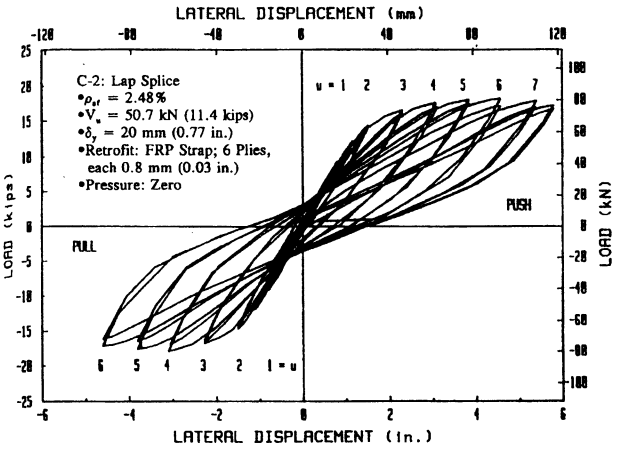

Fig. 9—Load-versus-displacement response of Column C-2

directions were slightly different for some of the test specimens. This difference affected the symmetries of the hysteresis loops.

In Fig. 8 through 12, V_u is the lateral force corresponding to the theoretical flexural capacity of the unconfined column section, δ_y is the yield displacement that was used as a reference value to determine each subsequent displacement ductility level that was applied to the specimen during the test, and ρ_{sl} is the longitudinal reinforcement ratio of the column. The measured and calculated maximum strengths for the retrofit and nonretrofit columns are summarized in Table 2. The calculated strength was determined using the procedures outlined in the ACI Code and taking into consideration the

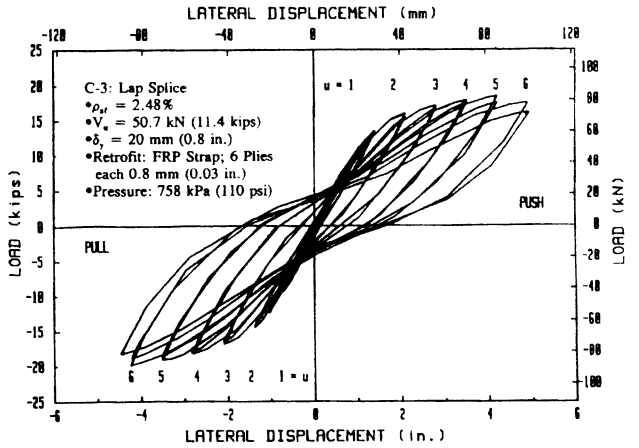

Fig. 10—Load-versus-displacement response of Column C-3

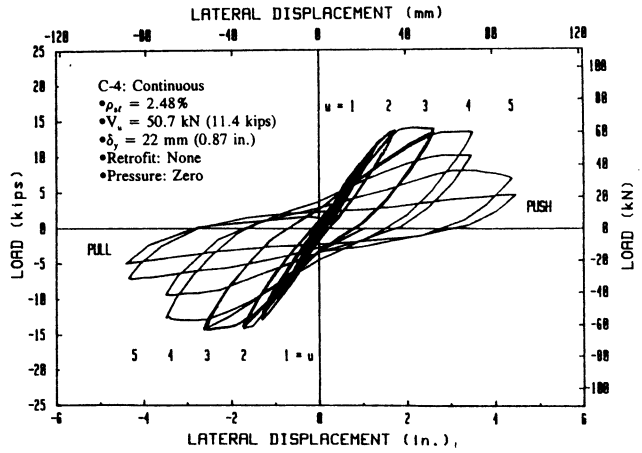

Fig. 11—Load-versus-displacement response of Column C-4

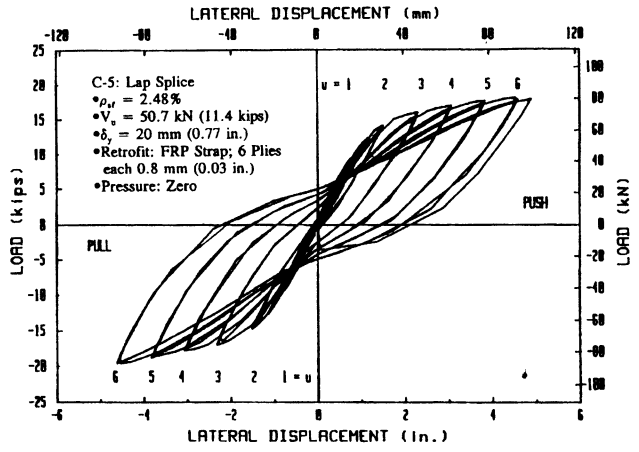

Fig. 12—Load-versus-displacement response of Column C-5

actual strain-hardening properties of the reinforcing steel. The percent increase in strength was calculated with reference to the measured value for the control specimen.

Fig. 8 shows that the hysteresis loops for the nonretrofit circular column (C-1) with lap splice reinforcement degrade rapidly after the first cycle to $u = 1.5$ due to the failure of the lapped reinforcement. The maximum lateral load of 58.3 kN (13.1 kips) was recorded during the push cycle to $u = 1.5$.

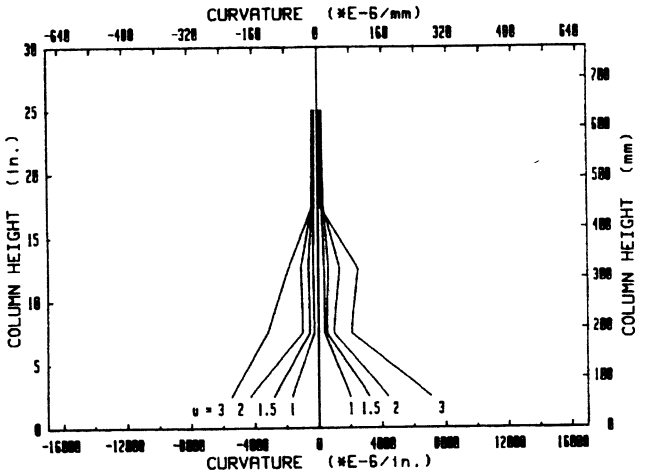

Fig. 13—Curvature-versus-height of Column C-1

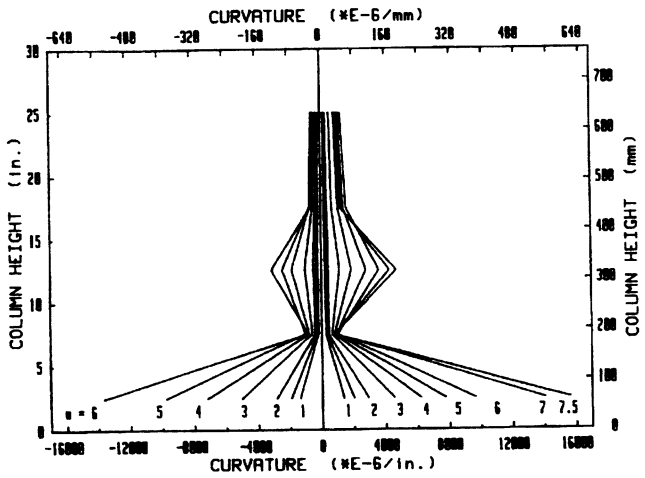

Fig. 14—Curvature-versus-height of Column C-2

The lateral responses of circular Columns C-2 and C-3, strengthened with six plies of FRP composite straps, applied with the passive and active retrofit schemes, respectively, show a significant improvement with stable hysteresis loops up to the displacement ductility level of $u = \pm 6$, as shown in Fig. 9 and 10. There was no sign of structural degradation of retrofit columns associated with the bond failure of lap-spliced bars. The maximum strength of 81.4 kN (18.3 kips) was noted for Column C-2. This value was approximately 40 percent higher than that of Reference Column (C-1). The increase in the maximum lateral load for Column C-3 was higher than that for Column C-2, perhaps due to the active confinement pressure.

Lateral load-displacement hysteresis loops for the two circular columns with continuous reinforcement are plotted in Fig. 11 and 12. Loops for the control specimen (C-4) in Fig. 11 show that the lateral strength did not decay until the displacement ductility level of $u = 4$. The maximum lateral load-carrying capacity was 71.6 kN (16.1 kips) at the displacement ductility level of $u = 3$. However, the specimen showed rapid deterioration in its strength at $u = 5$ due to concrete failure and longitudinal bar buckling. Fig. 12 shows hysteresis curves for Column C-5 with the passive retrofit scheme. These curves are very similar to those of Columns

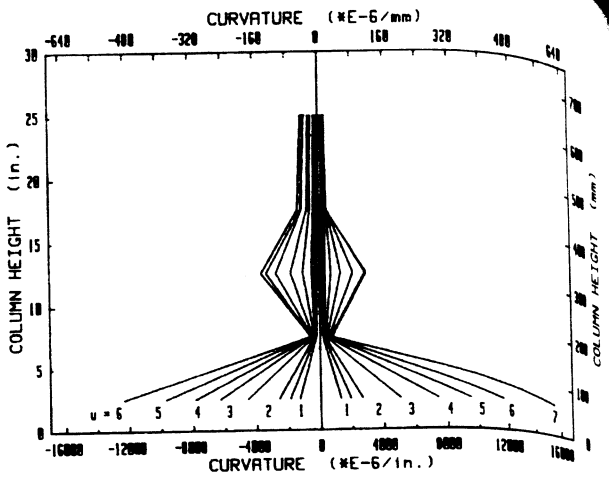

Fig. 15—Curvature-versus-height of Column C-3

C-2 and C-3, with significant improvement in strength and excellent energy absorption and dissipation characteristics.

Curvature-versus-height

Ten electrical inclinometers were mounted along the center line of each column on opposite faces (east and west), as shown in Fig. 7. The plastic rotation of specific sections of the column was then obtained from the readings of each inclinometer. An average curvature at the section was calculated from

$$\phi = \frac{\frac{(\theta_E + \theta_W)}{2}}{h_v} \quad (1)$$

where θ_E and θ_W are the east and west-side rotations of the cross section with respect to adjacent inclinometers, and h_v is the vertical distance between the adjacent inclinometers.

The vertical distributions of curvature within the plastic hinge region for the three circular columns with lapped starter bars are shown in Fig. 13 through 15. At the location of each of the clinometers, CL1 through CL5, shown in Fig. 7, the curvature was calculated and the corresponding points were connected by straight lines to show an approximate variation of the curvature within the plastic hinge region. The reduction in curvature from CL3 to CL4 is due to the fact that the reinforcement ratio is doubled within the splice region, resulting in a stiffer cross section. By comparing Fig. 13 and 14, one can see the increase in rotational capacity of the cross section resulting from the confinement provided by the composite strap. However, comparing Fig. 14 and 15 does not reveal measurable gain by actively confining the column. This could be partly due to the loss of the active pressure caused by seepage, creep, etc. The results from this test are not conclusive and additional tests are required to confirm the benefits of active retrofit. Fig. 16 and 17 show the curvature distribution within the confined portions of Columns C-4 and C-5, respectively. The comparison of these figures confirms the previous results, indicating the enhancement of ductility and rotational capacity of retrofit columns.

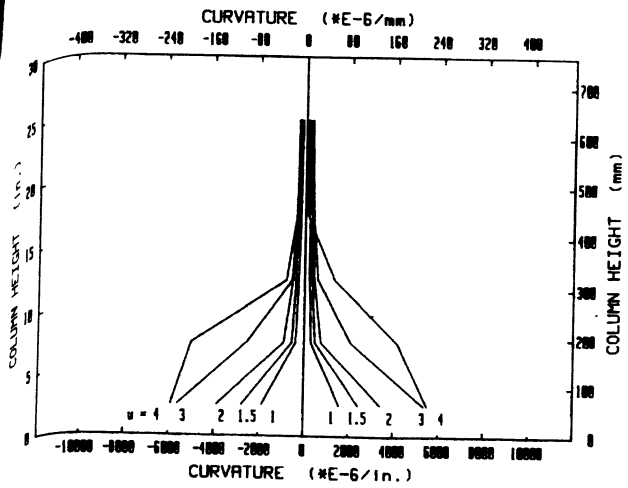

Fig. 16—Curvature-versus-height of Column C-4

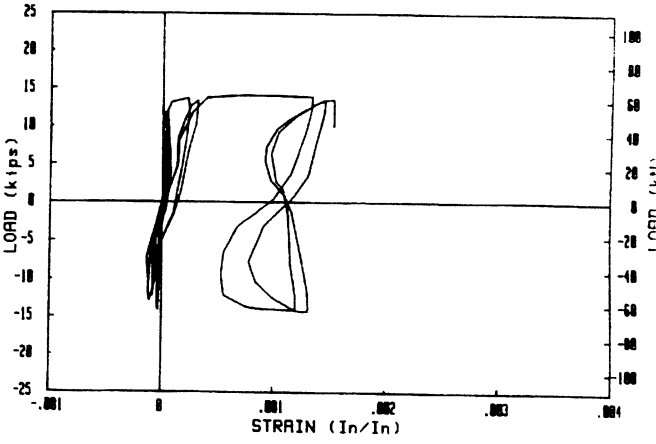

Fig. 18—Load-versus-strain in hoop of Column C-4

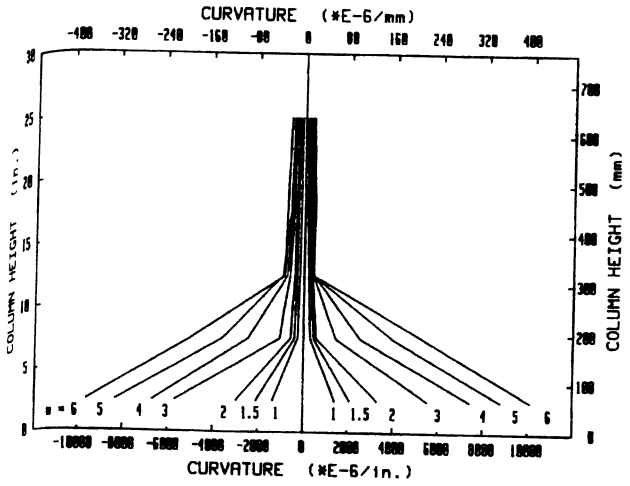

Fig. 17—Curvature-versus-height of Column C-5

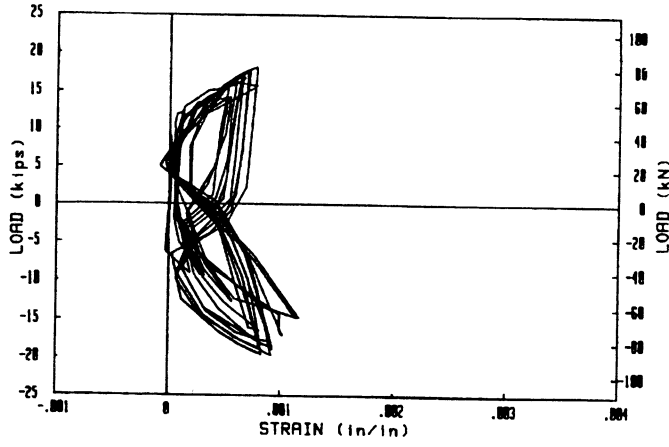

Fig. 19—Load-versus-strain in hoop of Column C-5 at Gage S8

Load-versus-strain

Longitudinal reinforcement

The measured maximum strain in longitudinal bars recorded at a location immediately above the top face of the footing on the extreme tension side of the columns for C-1, C-3, C-4, and C-5 were 21, 40, 35, and 53×10^{-4}, respectively. Due to the failure of the gages in Column C-2, the corresponding value for this column is not presented.

Generally, in the nonretrofit columns, the longitudinal reinforcements were less strained compared to retrofit columns. Factors contributing to this were the insufficient confinement, bond failure in the lapped starter bars, and/or buckling of continuous longitudinal bars in nonretrofit columns. Confinement by composite straps allowed higher strains in longitudinal reinforcements before failure, resulting in higher overall ductility and energy absorption capacity of the retrofit columns.

Transverse reinforcements

Lack of adequate lateral reinforcement will result in premature yielding of hoops and, therefore, loss of confinement and rapid deterioration of the plastic zone region. Strains in the column transverse reinforcements were recorded using special electric resistance strain gages mounted on opposite sides of the hoop wires. To compare the behavior of typical hoops in the retrofit and nonretrofit columns, the results of strain measurements at the same location for the first hoop above the footing of Columns C-4 and C-5 are presented herein. This hoop was approximately 30 mm (1.2 in.) above the top face of the footing. Fig. 18 and 19 show the load versus strain in the hoop for Columns C-4 and C-5, respectively. Normally, the hoops are in tension under the action of the applied loads. The slight compression strains shown in Fig. 18 and 19 are due to local effects at the location of the strain gages. In Column C-4, at the lateral load of approximately 62 kN (14 kips), the strain in the hoop reached 15×10^{-4}. However, at the same lateral load level, the strain in the retrofit Column C-5 was only 3×10^{-4}, indicating the effectiveness of the composite strap in sharing the load and confining and reducing the dilation of the core concrete.

Composite Strap

Strain gages were placed in the circumferential direction on the composite strap 572 mm (22.5 in.), 318 mm (12.5 in.),

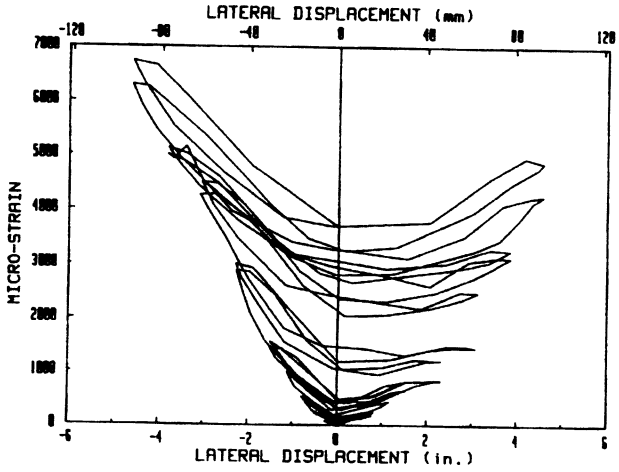

Fig. 20—Deflection versus strap-strain of Column C-2

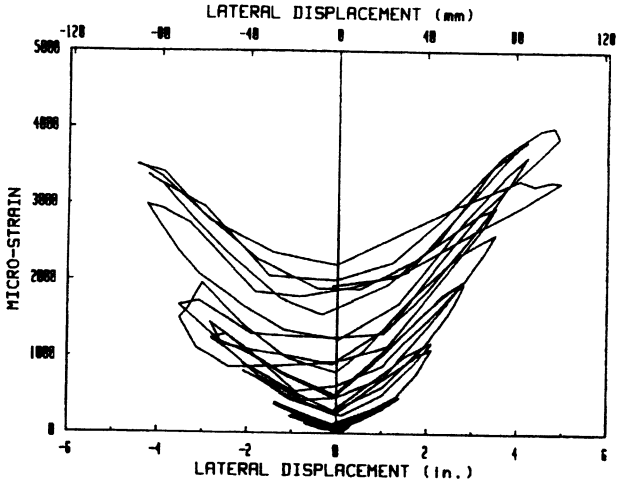

Fig. 21—Deflection versus strap-strain of Column C-3

and immediately above the top face of the footing on the extreme tension and compression sides of the cross section. Fig. 20 and 21 show the circumferential (hoop) strain in the composite strap measured with the strain gages immediately above the top face of the footing for Columns C-2 and C-3 versus applied lateral displacement. From these figures, it can be seen that the strains were increasing in magnitude as the displacement was increasing, even though the lateral loads were essentially constant after the displacement ductility reached the level of $u = 3$, which, on the average, for all these columns, approximately corresponded to a drift of 2.8 percent. The maximum strain reached in Column C-3 (active retrofit), not including the initial prestressing strain, is less than that of Column C-2 (passive retrofit), indicating that the initial pressure reduced the dilation of concrete. However, as was observed from the load-versus-displacement and load-versus-curvature responses, this reduced dilation indicated by the smaller strain in the composite strap with active retrofitting did not translate into measurable improvement in the overall ductility of the column.

Cracking and failure mechanisms

Since all of the specimens for this study were designed with a strong footing detail, most of the cracking damage in the control specimens was concentrated in the column, especially

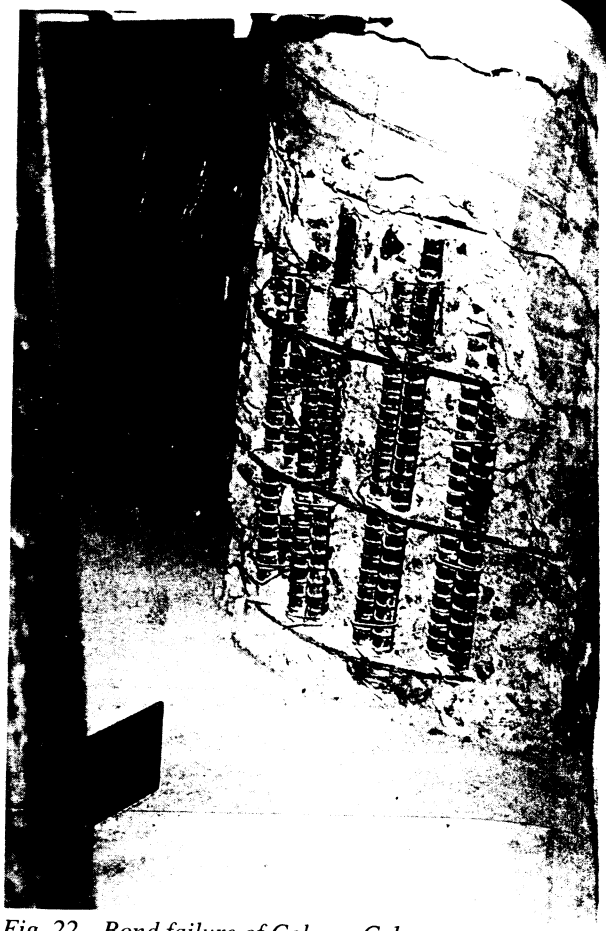

Fig. 22—Bond failure of Column C-1

within the plastic hinge region. The primary change of the behavior in Column C-1 occurred in the plastic hinge region at the displacement ductility level of $u = 1.5$. At this stage of the test, the cover concrete spalled and the longitudinal reinforcement bars started to debond in the lap-spliced region, as shown in Fig. 22. Column C-4 with continuous reinforcement started to fail at a displacement ductility level of $u = 4$. At this point, the longitudinal reinforcement started to buckle and the lateral load-carrying capacity reduced rapidly until complete failure of the column, as shown in Fig. 23.

CONCLUSIONS

The following conclusions are drawn based on the results of the tests conducted on reduced scale models of concrete bridge piers:

1. Reinforced concrete bridge columns, designed before the new seismic design provisions were in place, and with lap-spliced longitudinal reinforcement in the potential plastic hinge zone, appear to fail at low ductility levels of $u = 1.2$ to 1.5. This is due to the debonding of lapped starter bars, resulting from the lack of transverse reinforcement and insufficient development length of the longitudinal bars. The failure modes are brittle because strength deterioration is very rapid following debonding of longitudinal reinforcement.

2. For circular columns, the use of continuous reinforcement through the plastic hinge region improves moderately the lateral-displacement hysteresis loops. The structural degradation is likely to be delayed until ductility levels of $u = \pm 4$ are reached. The column failure is caused by longitudinal

reinforcement buckling within the hinge region due to the lack of lateral confinement.

3. Concrete columns externally wrapped with the FRP composite straps in the potential plastic hinge region showed a significant improvement in both strength and displacement ductility. The retrofit columns developed very stable load-displacement hysteresis loops up to a displacement ductility level of $u = \pm 6$, without evidence of significant structural deterioration associated with the bond failure of lapped started bars or longitudinal reinforcement buckling.

4. Both active and passive retrofit schemes provided additional confinement to existing core concrete, and were highly effective in preventing the columns from bond failure or longitudinal bar buckling, and hence, greatly increased the earthquake resistance of the column. The improvements resulting from the active retrofit scheme, as compared with the passive scheme, do not seem to justify the additional cost associated with the active retrofit scheme. This conclusion is, however, based on a limited number of tests. Additional studies are necessary to further investigate the benefits of active confinement.

ACKNOWLEDGMENTS

The research reported in this paper was sponsored by the National Science Foundation (NSF) through grants MSS 9022667 and MSS 9257344, Dr. John B. Scalzi, Program Director. The support of the NSF is greatly appreciated. The experimental work was conducted in the structural laboratories of the University of Arizona. Assistance from the technical staff of the laboratories is gratefully acknowledged.

REFERENCES

1. Thorkildsen, E., "Overview of Caltrans Bridge Seismic Research Program," *Proceedings of the 8th US-Japan Bridge Engineering Workshop*, Chicago, 1992, pp. 326-335.

2. New Zealand National Roads Board, *Research Bulletin* No. 71, Wellington, New Zealand, 1983.

3. Priestly, M. J. N., and Park, R., "Strength and Ductility of Reinforced Concrete Bridge Columns under Seismic Loading," *ACI Structural Journal*, V. 84, No. 1, Jan.-Feb. 1987, pp. 61-76.

4. Chai, Y. H.; Priestly, M. J. N.; and Seible, F., "Seismic Retrofit of Circular Bridge Columns for Enhanced Flexural Performance," *ACI Structural Journal*, V. 88, No. 5, Sept.-Oct. 1991, pp. 572-584.

5. Sun, Z.; Seible, F.; and Priestly, M. J. N., "Diagnostics and Retrofit of Rectangular Bridge Columns for Seismic Loads," *Proceedings of the 8th U.S.-Japan Bridge Engineering Workshop*, Chicago, 1992, pp. 282-296.

6. Priestly, M. J. N.; Seible, F.; and Fyfe, E., "Column Seismic Retrofit Using Fiberglass/Epoxy Jackets," *Proceedings of Advanced Composite Materials in Bridges and Structures*, Canadian Society for Civil Engineering, 1992, pp. 287-298.

7. Priestly, M. J. N.; Seible, F.; Xiao, Y.; and Verma, R., "Steel Jacket Retrofitting of Reinforced Concrete Bridge Columns for Enhanced Shear Strength—Part 2: Test Results and Comparison with Theory," *ACI Structural Journal*, V. 91, No. 5, Sept.-Oct. 1984, pp. 537-551.

8. Chambers, R. E., "Composites Performance in the Infrastructure," *Proceedings of Materials Science Conference*, ASCE, Atlanta, 1992, pp. 532-545.

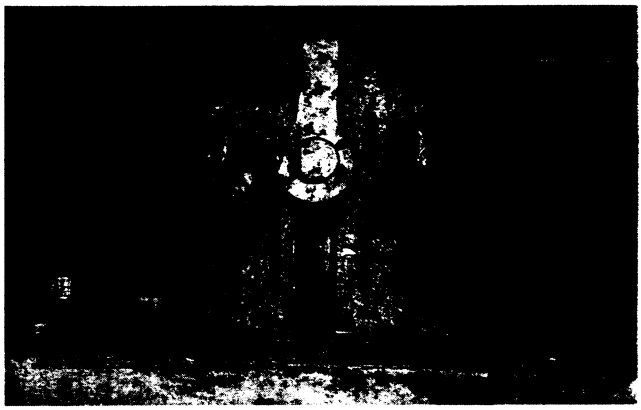

Fig. 23—Longitudinal bar buckling in Column C-4